Journal Pre-proof

Mono- and bimetallic (Pt/Cu) titanium(IV) oxide core-shell photocatalysts with UV/Vis light activity and magnetic separability

Zuzanna Bielan (Conceptualization) (Visualization) (Investigation) (Writing - original draft), Ewa Kowalska (Supervision) (Resources) (Writing - review and editing), Szymon Dudziak (Formal analysis) (Validation), Kunlei Wang (Investigation), Bunsho Ohtani (Supervision) (Resources), Anna Zielińska-Jurek (Conceptualization) (Supervision) (Writing - review and editing)

PII: S0920-5861(20)30315-1

DOI: https://doi.org/10.1016/j.cattod.2020.05.034

Reference: CATTOD 12884

To appear in: *Catalysis Today*

Received Date: 1 October 2019

Revised Date: 27 April 2020

Accepted Date: 7 May 2020

Please cite this article as: Bielan Z, Kowalska E, Dudziak S, Wang K, Ohtani B, Zielińska-Jurek A, Mono- and bimetallic (Pt/Cu) titanium(IV) oxide core-shell photocatalysts with UV/Vis light activity and magnetic separability, *Catalysis Today* (2020), doi: https://doi.org/10.1016/j.cattod.2020.05.034

Mono- and bimetallic (Pt/Cu) titanium(IV) oxide core-shell photocatalysts with UV/Vis light activity and magnetic separability

Zuzanna Bielan[a,b,*] , Ewa Kowalska[b], Szymon Dudziak[a], Kunlei Wang[b], Bunsho Ohtani[b], Anna Zielińska-Jurek[a]

[a] *Department of Process Engineering and Chemical Technology, Chemical Faculty, Gdansk University of Technology, 80-233 Gdansk, Poland*

[b] *Institute for Catalysis (ICAT), Hokkaido University, N21, W10, 001-0021 Sapporo, Japan*

* Corresponding author Tel.: + 48 58 347 13 90 (ZB)

e-mail address: bielan_chan@onet.eu (ZB)

Graphical abstract

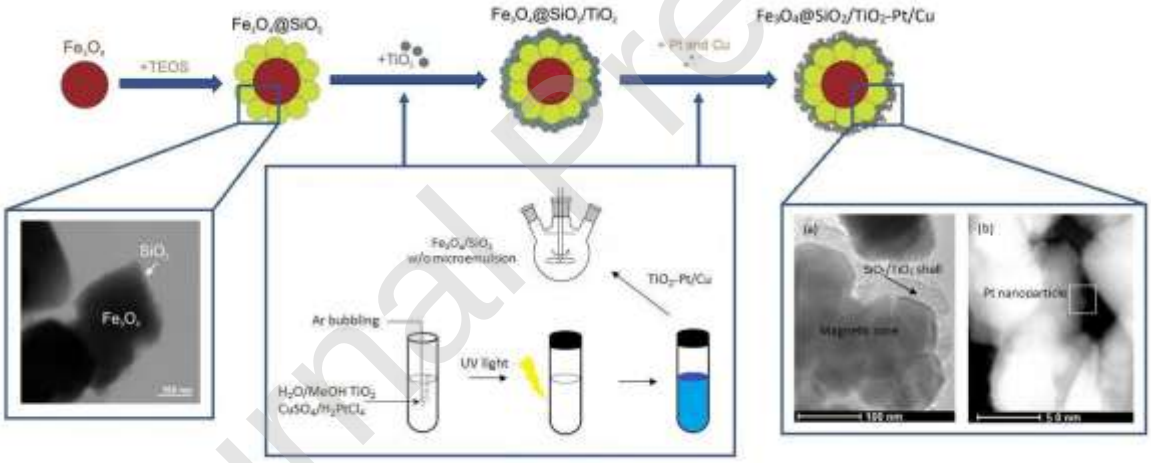

Highlights

- Preparation of magnetically separable $TiO_2/SiO_2/Fe_3O_4$ nanocomposites
- Core-interlayer-shell structure of bimetal-modified magnetic photocatalysts
- High photocatalytic activity of metal-modified magnetic photocatalysts
- $Fe_3O_4@SiO_2/TiO_2$-M revealed high stability after subsequent cycles of degradation

Abstract

Titanium(IV) oxide is one of the most widely investigated photocatalysts. However, separation of nano-sized particulate titania might result in profitless technologies for commercial applications. Additionally, bare titania is almost inactive under the Vis range of solar spectrum due to its wide bandgap. Therefore, the present study aims to prepare novel core-interlayer-shell TiO_2 magnetic photocatalysts modified with metal nanoparticles (Pt, Cu), which exhibit both photocatalytic and magnetic properties, making it easily separable within the magnetic field. Accordingly, the core-shell structure of Fe_3O_4@SiO_2/TiO_2 was obtained in water/TX100/cyclohexane microemulsion. Platinum and copper were photodeposited on four TiO_2 templates and characterized by X-ray diffractometry (XRD), X-ray photoelectron spectroscopy (XPS), specific surface area (BET) measurement and diffuse reflectance spectroscopy (DR-UV/Vis). Photoactivity was studied in the reaction of phenol, acetic acid, and methanol degradation under UV/Vis irradiation, using both polychromatic and monochromatic irradiation (action spectrum analysis). The core-interlayer-shell structure of Pt and Cu modified magnetic photocatalysts was confirmed using scanning transmission electron microscopy (STEM). Magnetic photocatalysts modified with platinum and copper revealed improved photoactivity both in oxidation and reduction photocatalytic reactions, as compared to unmodified Fe_3O_4@SiO_2/TiO_2 photocatalysts. Finally, the correlation between physicochemical properties and photocatalytic activities of Fe_3O_4@SiO_2/TiO_2-Pt/Cu photocatalysts was investigated. For the first time, the effect of metals' loading on the efficiency of phenol degradation and mineralization (TOC removal), and quantum efficiency of reaction in the presence of magnetic photocatalysts were analyzed. It was found that phenol can be

efficiently decomposed (ca. 100%) during 60 min of UV/Vis irradiation for the photocatalyst recovered within the magnetic field during three subsequent degradation cycles.

Keywords: Pt-Cu-modified magnetic photocatalyst, core-shell structure, quantum efficiency, magnetic separation, titania

1. Introduction

In recent years, the importance of photocatalysis using TiO_2 nanoparticles has been increasing in various fields, e.g., wastewater treatment [1], air purification [2], and energy conversion [3], due to their low price, stability, chemical inertness and high photocatalytic efficiency. Nevertheless, there are three limitations to the scaling-up of titania photocatalytic reactions. Firstly, TiO_2 is activated almost only by ultraviolet (UV) light, due to its wide bandgap (ca. 3.0-3.2 eV, depending on polymorphic form) [4–6]. Therefore, the application of artificial irradiation sources (UV lamps) instead of sunlight radiation might increase the costs of the purification process.

The second shortcoming of titania, typical for all semiconductors, is the fast recombination of charge carriers, resulting in much lower than expected quantum yields of photocatalytic reactions. In this regard, much attention has been paid to increase the light absorption in the visible range and to inhibit the recombination rate. Various methods of titania modifications have been proposed, such as surface modification with noble metals (Pt, Ag, Au, Pd) [7–10], doping with non-metals (N, S, C, P, B, I, F) [11–16], heterojunction with other semiconductors [17,18] and sensitization with color compounds (e.g., dyes [19]). Among them, surface modification with noble metals has been the most prevalent since A. Bard [20] introduced it for enhancement of activity under UV irradiation. Recently, noble metal nanoparticles have been used for titania modification to absorb visible light due to localized surface plasmon resonance (LSPR) properties [21,22]. Moreover, the deposition of metallic nanoparticles on the TiO_2 surface could increase photocatalytic activity by (i) reducing the electron-hole recombination,

(ii) increasing the efficiency of interfacial charge transfer, and (iii) generating charge carriers due to light interaction [23–27]. However, the addition of high content of noble metals (1-5%), mainly platinum and gold, could also generate high costs of photocatalyst preparation and even result in an activity decrease due to the "shielding effect." Hence, it is possible to reduce the amount of expensive noble metals by creating bimetallic systems with cheaper metals, e.g., copper or silver [28,29], which also can enhance photocatalytic activity due to synergistic effect between both metals [30–32].

The third challenge in photocatalysis is a separation of semiconductor nanoparticles from post-process suspension. Owing to nanometric particle size, TiO_2 could be detached from the photocatalytic batch system almost only by highly expensive ultrafiltration [33,34]. Alternatively, nanoparticles have been immobilized on solid substrates, such as glass, sand, ceramic balls, zeolites, activated carbon, or optical fibers [35]. However, it should be pointed out that photocatalyst immobilization usually results in a significant decrease in specific surface area and thus decrease in photocatalytic activity. For example, Zielińska-Jurek et al. showed that TiO_2 activity decreased by ca. 30% after its impregnation on a glass substrate [36]. Moreover, the immobilized TiO_2 layer is often unstable, and due to abrasion might be detached during the photocatalytic reactions [37,38]. Therefore, other methods of photocatalyst recovery have been intensively investigated, and magnetic separation is considered as the most prospective. For example, the modification of titanium(IV) oxide with Fe_3O_4 [39,40] and γ-Fe_2O_3 [41,42], as well as other compounds exhibiting magnetic properties [43–45] has been proposed for effective photocatalyst separation from the reaction suspension.

Considering these limitations, in this study, the modification of magnetic titania photocatalyst with noble/semi-noble metals has been proposed, which should result in the preparation of highly active photocatalyst at a wide range of irradiation and easily separation. In the last years, only a few reports regarding metal modified TiO_2 loaded on a magnetic core

material have been reported. For example, Li et al. [46] prepared hierarchical Fe_3O_4@SiO_2@TiO_2@Pt photocatalyst with highly active nanoplatelets of titania with exposed (001) facets. As a photocatalytic shell, Ag-modified TiO_2 was also used [47,48]. However, mono- and bimetal modification of various titanium(IV) oxide templates loaded on magnetic cores has not been reported yet. Moreover, the majority of the reported studies for the photocatalytic activity of magnetic nanocomposites were investigated in the reaction of organic dyes degradation [49–53], which has been considered as unsuitable due to sensitization mechanism by dyes [54,55].

Therefore, the aim of the present study was preparation and characterization of the mono- and bi-metal modified TiO_2 photocatalysts of different polymorphic compositions, additionally deposited on magnetic particles (Fe_3O_4), forming a core-shell structure. An inert silica layer in the structure of the magnetic photocatalyst was introduced to prevent leaching of iron ions into the solution. The effect of noble and semi-noble metals' loading, TiO_2 template on photooxidation of phenol, acetic acid, and methanol dehydrogenation was investigated. Furthermore, for the first time for metal-modified TiO_2 matrices embedded on a magnetic core, quantum efficiency was determined in the phenol oxidation reaction under monochromatic irradiation in the range of 320-620 nm.

2. Materials and methods

Commercial titania samples: ST01 (ST-01, Ishihara Sangyo, Osaka, Japan), ST41 (ST-41, Ishihara Sangyo), and FP6 (Showa Denko K.K., Tokyo, Japan) were supplied as photocatalysts' shell matrix. Other chemicals, including titanium n-butoxide (TBT, 96.0%), cetyltrimethylammonium bromide (CTAB, 98%), magnetite (Fe_3O_4, particles size of about 50 nm, 97%), tetraethyl orthosilicate (TEOS, 99%), chloroplatinic acid hexahydrate (99%), copper(II) sulfate (99.9%), cyclohexane, acetone, methanol, 2-propanol, acetic acid, ammonium hydroxide solution (25%), acetonitrile (HPLC grade), phosphoric acid (HPLC

grade, 85%) and phenol (99.5%) were purchased from Wako Pure Chemicals (Osaka, Japan). All materials were used as received without further purification.

2.1. Preparation of TiO_2-M photocatalysts

Four different types of titania (commercial: ST01, ST41 and FP6, and self-prepared TBT - from titanium n-butoxide hydrolysis) were modified with platinum and/or copper nanoparticles using photodeposition method. The complete procedure was described in our Data in Brief article [56].

2.2. Preparation of magnetic Fe_3O_4@SiO_2/TiO_2-M photocatalysts

The TiO_2-M nanoparticles were deposited on spinel ferrite particles as a thin photocatalytic active shell. Magnetite (Fe_3O_4) was chosen as a core of the designed composite due to its high magnetic properties, which enables to separate obtained photocatalyst in an external magnetic field. Silica was used as an inert interlayer to isolate Fe_3O_4 from TiO_2 and suppress possible electron transfer between them. The magnetic photocatalysts were obtained in w/o microemulsion system based on changes in the particles' surface charge as a function of pH value, which was described in previously published work [57].

In the first part, commercially available Fe_3O_4 nanoparticles with nominate particles diameter of about 50 nm were dispersed in water at pH 10. After this, the prepared suspension was introduced to cyclohexane/isopropanol (100:6 volume ratio) solution in the presence of cationic surfactant, cetyltrimethylammonium bromide (CTAB), creating stable w/o microemulsion system with water nanodroplets dispersed in the continuous oil phase. The molar ratio between water and surfactant content was set at 30. After 2 h of microemulsion stabilization, a corresponding amount of tetraethyl orthosilicate (TEOS) and precipitating agent (ammonia) were added into the microemulsion, resulting in the formation of SiO_2 interlayer. The molar ratios of TEOS to Fe_3O_4 and NH_4OH to TEOS were 8:1 and 16:1, respectively. After 12-h mixing, microemulsion was destabilized by acetone addition and obtained nanocomposite

Fe_3O_4@SiO_2 was separated, washed with ethanol and water, dried at 70 °C to dry mass and calcined at 400 °C for 2 h. Two different types of Fe_3O_4@SiO_2 magnetic matrices were synthesized, marked as z2 and z3, differing by the adding order of TEOS and ammonia, i.e., NH_4OH first and TEOS first, respectively.

In a second step, previously obtained Fe_3O_4@SiO_2 particles were coupled with pure TiO_2 or TiO_2-M to create photocatalytically active shells. As previously, a reversed-phase microemulsion system at pH 10 was used. The Fe_3O_4:TiO_2 molar ratio was set to 1:2. The junction between the magnetic/silica core and the photocatalytic layer was promoted by their opposite surface charges, provided by the presence of CTAB at basic pH. Fe_3O_4@SiO_2/TiO_2 and Fe_3O_4@SiO_2/TiO_2-M samples, after their separation and purification using water and ethanol, were dried at 70 °C to dry mass and calcined at 400 °C for 2 h.

2.3. Characterization of obtained photocatalysts

XRD analyses were performed using the Rigaku Intelligent X-ray diffraction system SmartLab (Tokyo, Japan) equipped with a sealed tube X-ray generator (a copper target; operated at 40 kV and 30 mA). Data were collected in the 2θ range of 5-80°. Scan speed and scan steps were fixed at $1^{o}\cdot min^{-1}$ and 0.01°, respectively. The analysis was based on the International Centre for Diffraction Data (ICDD) database. The crystallite size of the photocatalysts in the vertical direction to the corresponding lattice plane was determined using Scherrer's equation, with Scherrer's constant equals 0.891. Quantitative analysis, including phase composition with standard deviation, was calculated using the Reference Intensity Ratio (RIR) method from the most intensive independent peak of each phase.

Nitrogen adsorption-desorption isotherms (BET method for the specific surface area) were recorded using the Micromeritics Gemini V (model 2365) (Norcross, GA, USA) instrument at 77 K (liquid nitrogen temperature).

The light-absorption properties were measured using diffuse reflectance (DR) spectroscopy, and the data were converted to obtain absorption spectra. The bandgap energy of photocatalysts was calculated from the corresponding Kubelka-Munk function, $F(R)^{0.5}E_{ph}^{0.5}$ against E_{ph}, where E_{ph} is photon energy. The measurements were carried out on JASCO V-670 (Tokyo, Japan), equipped with a PIN-757 integrating sphere. As a reference, BaSO4 or respective bare titania was used.

Samples morphology, as well as core-shell structures formation, were determined by scanning transmission electron microscopy (STEM) equipped with energy-dispersive X-ray spectroscopy (EDS; HITACHI, HD-2000, Tokyo, Japan).

The oxidation states of elements, especially platinum and copper, were determined by XPS measurements on JEOL JPC-9010MC X-ray spectrometer (JEOL Ltd, Tokyo, Japan).

2.4. Measurements of photocatalytic activity

Photocatalytic activity of obtained samples was evaluated in three reaction systems: (1) phenol degradation reaction under UV-Vis irradiation, (2) decomposition of acetic acid under UV-Vis irradiation, and (3) dehydrogenation of methanol under UV-Vis irradiation. For phenol degradation reaction, the 300 W xenon lamp (LOT Oriel, Darmstadt, Germany) was used. A 0.05 g (1 g·dm^{-3}) of a magnetic nanocomposite, where 0.02 g corresponds to photocatalytic active TiO_2, together with 20 mg·dm^{-3} phenol solution was added to 50 cm^3 quartz photoreactor with an exposure layer thickness of 3 cm, and obtained suspension was stirred in darkness for 30 min to provide adsorption-desorption stabilization. After equilibrium was established, photocatalyst suspension was irradiated (60 mW·cm^{-2}) for 60 min under continuously stirring. The constant temperature of the aqueous phase was kept at 20 °C using a thermostated water bath. Every 10 min of irradiation, 1.0 cm^3 of suspension was collected and filtered through a syringe filter (pore size: 0.2 µm) for the removal of photocatalysts particles. The concentration of phenol and formed intermediates was estimated using a reversed-phase high-performance

liquid chromatography (HPLC) system, equipped with a C18 chromatography column with bound residual silane groups (Phenomenex, model 00F-4435-E0) and a UV-Vis detector with a DAD photodiodes array (model SPD-M20A, Shimadzu). The tests were carried out at 45 °C and under isocratic flow conditions of 0.3 $ml \cdot min^{-1}$ and volume composition of the mobile phase of 70% acetonitrile, 29.5% water, and 0.5% orthophosphoric acid. Qualitative and quantitative analysis was performed based on previously made measurements of relevant substance standards [58] and using the method of an external calibration curve. Total organic carbon (TOC) was measured using TOC-L analyzer (Shimadzu, Kyoto, Japan).

For acetic acid decomposition, 0.05 g of nanocomposite (including 0.02 g of pure or metal-modified TiO_2) was suspended in 5 cm^3 of 5 vol% aqueous acetic acid solution. The 30 cm^3 testing tube with as prepared suspension was sealed with a rubber septum and irradiated for 60 min using the 400 W mercury lamp (Hamamatsu Photonics, Hamamatsu, Japan) under continuous stirring and temperature control. Every 20 min, liberated CO_2 in a gas phase was estimated chromatographically using a Shimadzu GC-8A Chromatograph (Shimadzu Corporation, Kyoto, Japan) equipped with thermal conductivity detector (TCD) and Porapak Q column (Agilent Technologies, Santa Clara, CA, USA).

For methanol dehydrogenation, 0.05 g of nanocomposite (0.02 g of TiO_2) was suspended in 5 cm^3 in methanol-water solution (volume ratio 50:50). The obtained suspension was first purged with argon for oxygen removal, and the testing tube was sealed with a rubber septum and irradiated for 1 h using mercury lamp (same reaction system as that used for acetic acid decomposition). Generated hydrogen was determined every 15 min using a Shimadzu GC-8A Chromatograph with TCD detector and MS-5A column (Agilent Technologies).

Additional photoactivity measurements for pure TiO_2 matrices and unmodified $Fe_3O_4@SiO_2/TiO_2$ nanocomposites were performed in reaction of 4-nitrophenol reduction to 4-aminophenol, based on the studies by Imamura et all. [59] and Brezova et all. [60]. To 50 cm^3

quartz photoreactor, 0.1 g (1 g·dm^{-3}) of pure TiO_2 or magnetic nanocomposite, where 0.04 g corresponds to photocatalytic active TiO_2, was added together with 50 cm^3 500 μM 4-nitrophenol solution in methanol. Oxygen was removed from suspension using nitrogen purging. After complete oxygen removal, the mixture was irradiated for 1 h using 300-W xenon lamp with light intensity set to 30 mW·cm^2. Every 10 min, 1.0 cm^3 of suspension was collected, filtered through a syringe filter, and analyzed using high-performance liquid chromatography (HPLC) system. The measurement of 4-nitrophenol and 4-aminophenol concentration was performed at 45 °C and under isocratic flow conditions of 1 cm^3·min^{-1} and volume composition of the mobile phase of 60% water, 39.5% acetonitrile and 0.5% orthophosphoric acid.

2.5. Quantum efficiency of photocatalytic phenol degradation

Apparent quantum efficiency was determined in phenol oxidation reaction under monochromatic irradiation. The generation of 1,4-benzoquinone (BQ; intermediate phenol product) was quantified at seven irradiation wavelengths: 320, 380, 440, 450, 500, 560, and 620 nm. 0.03 g of nanocomposite (0.012 g of photocatalytic active TiO_2) and 3 cm^3 of phenol solution (c = 20 mg·dm^{-3}) were placed in a quartz cuvette and irradiated with monochromatic light emitted by a diffraction grading type illuminator Jasco CRM-FD (Jasco Corporation, Tokyo, Japan). Irradiation intensity was set in the range of 7.2 - 9.9 mW·cm^{-2} and measured using a Hioki 3664 Optical Power Meter (Hioki EE Corporation, Nagano, Japan). The concentration of formed BQ was determined chromatographically using the Shimadzu LC-6A system equipped with the WAKOSIL-II 5C18 AR column (FUJIFILM Wako Pure Chemical Corporation, Osaka, Japan) and a UV-Vis detector (model SPD-6A, Shimadzu). The tests were performed at 45 °C and under isocratic flow conditions of 1 cm^3·min^{-1} and volume composition of the mobile phase of 70% water, 29.5% acetonitrile, and 0.5% orthophosphoric acid. The detection wavelength was set at 254 nm.

3. Results and discussion

3.1. Physicochemical characterization of obtained nanocomposites

Exemplary XRD patterns for Fe_3O_4@SiO_2/TiO_2-M samples are presented in Fig.1a-b with detailed crystal phase composition and crystallite sizes for all samples being listed in Tables S1-S6 in Supplementary Material. For magnetic composites, the presence of crystalline phases of both magnetite and TiO_2 was detected in all patterns, with the diffraction peaks for Fe_3O_4 inverse cubic spinel structure at 30.1°, 35.6°, 43.3°, 57.2°, 62.8° (ICDD card No 9002319) and anatase as main TiO_2 polymorph at 25°, 37.8°, 47.9°, 53.8°, 54.9°, 62.6°, 68.7° and 70° (ICDD card No 9009086). The content of magnetite crystalline phases varied from 28.3% to 35% for ST01 and FP6 samples, respectively, for composites without deposited metals. For Fe_3O_4@SiO_2/TBT-M nanocomposites, in opposite to previously described TiO_2-M [56], the brookite phase was not detected probably due to additional thermal annealing process after preparation of the core-shell structure of magnetic photocatalyst. Interestingly, the content of the rutile phase in the FP6 sample decreased significantly after the preparation of magnetic nanocomposites. For example, the anatase to rutile ratio increased from 3.6 for bare FP6 sample to 45.7 for magnetic composite containing 0.5% Cu ([56] and Table S4 in Supplementary Material). Therefore, brookite – anatase transition, as well as amorphous phase – anatase transition related to additional calcination of Fe_3O_4@SiO_2/TiO_2-M nanocomposites, is proposed as one of the possibilities [61]. The presence of amorphous silica was confirmed by enlargement of the patterns between 15 and 25 reflection angles [53,62]. The presence of platinum and copper was not approved by XRD analysis (no peaks for platinum or copper) due to their low content (0.05-0.5 mol%) and nanometric size. No other crystalline phases were identified in the patterns, which indicated the crystal purity of the obtained composites.

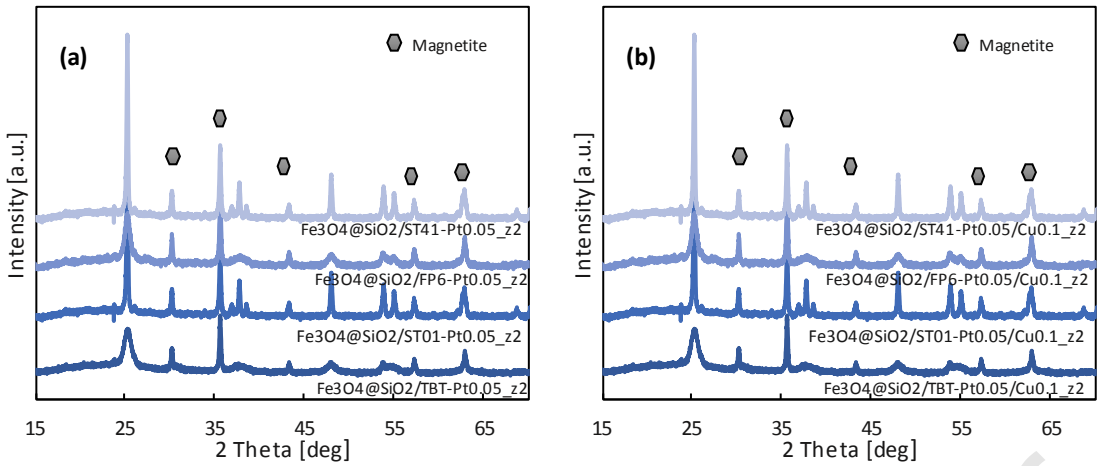

Fig. 1. XRD patterns of mono-metal (a) and bi-metal (b) Fe_3O_4@SiO_2/TiO_2-M magnetic photocatalysts

The photoabsorption properties of the prepared magnetic materials were studied by diffuse reflectance spectroscopy, and exemplary data are shown in Fig. 2. As a representative for magnetic nanocomposite, Fe_3O_4@SiO_2/TBT-Pt0.05_z2 was compared with the metal-modified TBT matrix. The light absorption was extended in the range above 400 nm for the obtained nanocomposites. Previously, the red-shifted light absorption was observed for TiO_2-SiO_2 shell coating the magnetic core [63]. The absorption at the Vis range for TBT-Cu0.5 and TBT-Pt0.05, presented by Bielan et al. [56], confirmed that noble metals were successfully deposited on the titania surface. Although for platinum the plasmonic peaks could be observed for all Pt-modified samples (spectra with bare titania as a reference) with maximum absorption at ca. 380-420 nm [64], the copper exists as an oxidation state-mixed form (i.e., zero-valent, Cu_2O and CuO), because of its easy oxidation in air, as already reported for other Cu-modified titania samples [65,66].

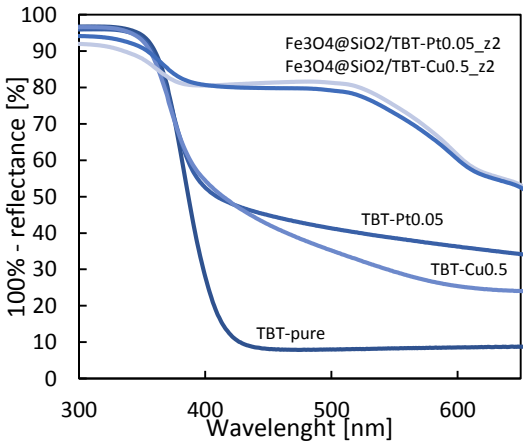

Fig. 2. Exemplary DR-UV/Vis spectra of nanocomposites with $BaSO_4$ as a reference.

The specific surface area (BET) data for the obtained magnetic core-shell titania-based nanocomposites are presented in Tables S7-S8 in the Supplementary Materials. After introducing titania photocatalyst (bare or modified) on the Fe_3O_4@SiO_2 magnetic core, the specific surface area increased significantly due to the presence of a highly porous silica interlayer (Table S7). It was found that the highest BET for monometallic samples was obtained for magnetic nanocomposites modified with 0.05 mol% of Pt reaching 160, 170, 110, and 119 $m^2 \cdot g^{-1}$ for TBT, ST01, FP6, and ST41, respectively, suggesting the presence of non-aggregated fine nanoclusters of platinum. There was no meaningful difference between the BET specific surface area of mono- and bimetallic magnetic nanocomposites.

The STEM analyses were performed to confirm the core-shell structure as well as the presence of platinum and copper on the titania surface. The exemplary results for Fe_3O_4@SiO_2/TBT-Pt0.05_z2 sample as a representative magnetic nanocomposite are presented in Fig. 3.

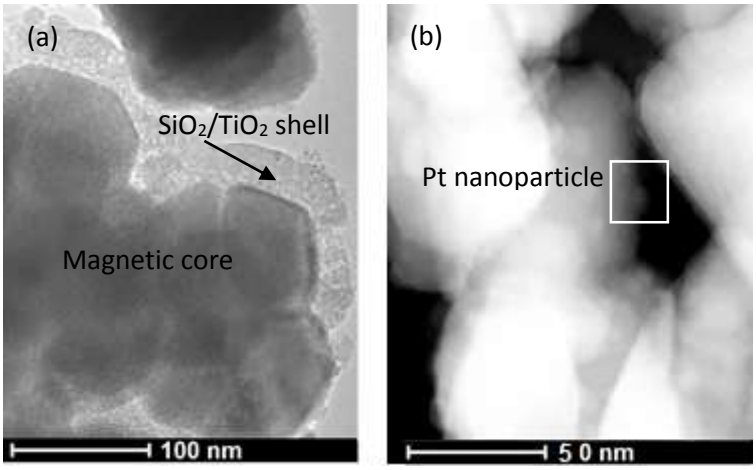

Fig. 3. STEM images of Fe_3O_4@SiO_2/TBT-Pt0.05_z2 nanocomposite

The analysis confirmed the formation of a photocatalytic coating on the magnetic Fe_3O_4 core. Magnetite particles with a size of about 50 nm tended to agglomerate, which led to creating about 20 nm SiO_2/TiO_2 shell on the entire agglomerated surface. Pt nanoparticles of the average diameter smaller than 10 nm were uniformly distributed on the surface.

The surface properties and oxidation state of elements were investigated by X-ray photoelectron spectroscopy (XPS), and the obtained results for three different magnetic nanocomposites containing ST01 titania shell are shown in Table 1 and Fig. 4.

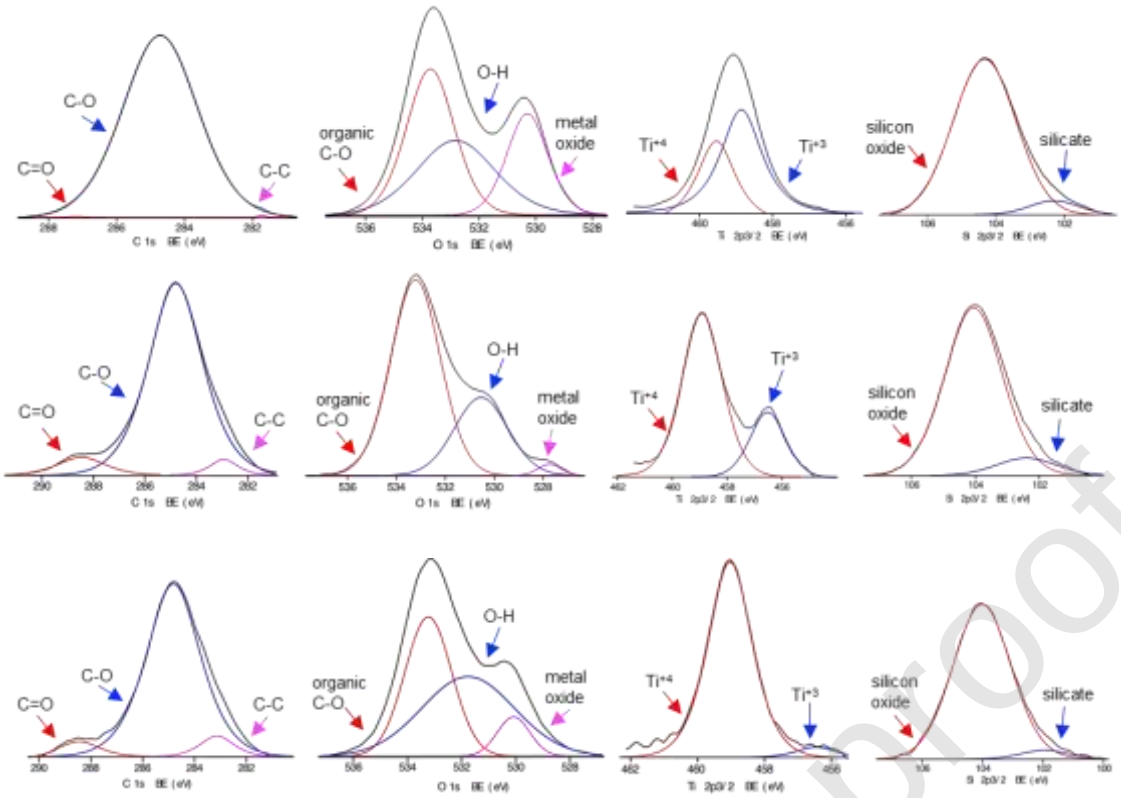

Fig. 3. Deconvolution of X-ray photoelectron spectroscopy (XPS) spectra for C 1s, O 1s, Ti $2p_{3/2}$ and Si $2p_{3/2}$ for Fe_3O_4@SiO_2/ST01-s_z2, Fe_3O_4@SiO_2/ST01-Pt0.05_z2 and Fe_3O_4@SiO_2/ST01-Pt0.05/Cu0.1_z2 samples (from the top)

Table 1. X-ray photoelectron spectroscopy (XPS) analysis of Ti, O, C, Fe, Si, Pt and Cu

Sample	Content (at.%)						
	Ti 2p	O 1s	C 1s	Fe 2p	Si 2p	Pt 4f	Cu 2p
Fe_3O_4@SiO_2/ST01-s_z2	3.12	34.07	50.36	1.87	10.59	-	-
Fe_3O_4@SiO_2/ST01-Pt0.05_z2	8.21	50.56	24.15	0.09	16.96	0.04	-
Fe_3O_4@SiO_2/ST01-Pt0.05/Cu0.1_z2	3.34	36.58	48.85	0.02	10.97	0.11	0.11

Although the same content of platinum was used for modification, the surface content of platinum was almost three times higher in the magnetic bimetallic nanocomposite, which might suggests that co-deposition of copper could result in formation of larger nanoparticles than that in the case of simple Pt deposition on fine titania (probably nano-sized Pt clusters). The presence of copper was confirmed in the bimetallic sample, reaching 0.11 at. %. Iron content

ranged from 0.02 at.% for Fe_3O_4@SiO_2/ST01-Pt0.05/Cu0.1_z2 to 1.87 at.% for Fe_3O_4@SiO_2/ST01-s_z2, which was expected for core-shell nanostructure, and confirmed that the core was composed of magnetite. The Fe 2p signal was deconvoluted into 709 and 711 eV peaks, corresponding to FeO and Fe_2O_3 co-present in magnetite. The comparison between magnetic samples also suggested that platinum might replace oxygen (the smallest O/(Ti+Si) ratio), as already published for other titania samples [50]. Interestingly, the highest O/(Ti+Si) ratio for bimetallic magnetic composite confirmed the presence of copper oxides rather than zero-valent copper. The Ti 2p peak could be divided into 456 eV and 459 eV binding energies and identified as Ti^{3+} and Ti^{4+}, respectively. Ti^{4+} was a dominant surface state for the most samples. However, it should be pointed out that the Ti^{3+} content in magnetic composites was quite high, suggesting titanium reduction during the microemulsion method. Silicon (Si 2p) appeared in two forms: silicate (102 eV) and silicon oxide (104 eV), among which SiO_2 state is dominant (90-96%). Carbon was detected in all analyzed samples and varied from 24.15 to even 50.36 at.%, which is typical for all titania (and others) samples, and mainly originated from carbon(IV) oxide adsorption from surrounding air.

The oxygen to titanium and titanium/silicon ratio exceeded the expected one (2.0 considering only SiO_2 and/or TiO_2, as Fe_3O_4 core is almost undetectable) for nearly all analyzed samples, reaching 2.5, 2.0 and 2.6 for ST01: bare on magnetic core, modified with 0.05 mol% Pt on magnetite and modified with 0.05 mol% Pt and 0.1 mol% Cu on magnetic core, respectively. The enrichment of the surface with oxygen (mainly in the form of hydroxyl groups) is common and often reported for different titania photocatalysts [67].

3.2. Photoactivity of mono- and bimetallic Fe_3O_4@SiO_2/TiO_2 nanocomposites

Firstly, photoactivity of core-shell non-metal modified Fe_3O_4@SiO_2/TiO_2 nanocomposites was studied in methanol dehydrogenation and acetic acid decomposition. The obtained results, in comparison with pure TiO_2 matrices, are shown in Fig. 5a-d.

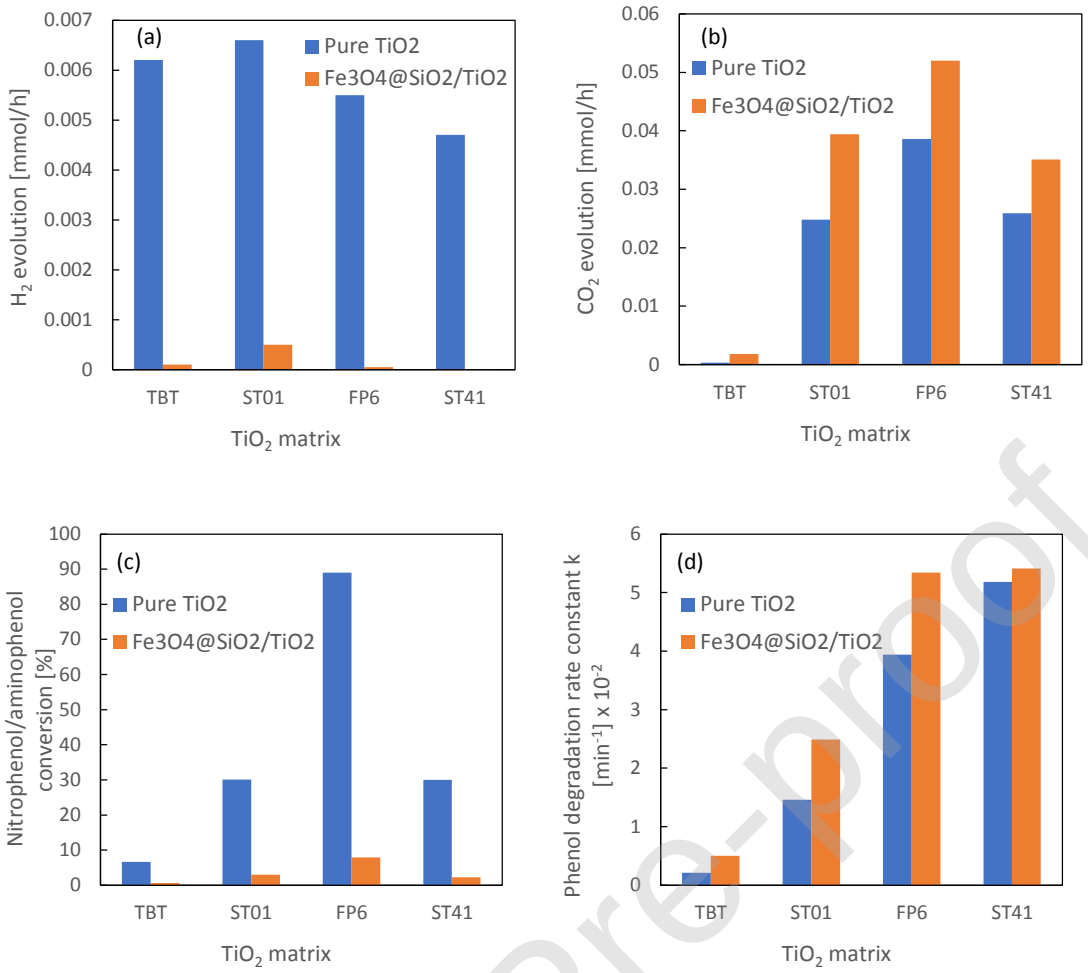

Fig. 5. H_2 evolution (a) and acetic acid oxidation to CO_2 (b) as well as nitrophenol/aminophenol conversion percentage (c) and phenol oxidation rate constant k (d) as a function of TiO_2 matrix for pure TiO_2 and Fe_3O_4@SiO_2/TiO_2 nanocomposites

Performed observations remained similar to pure TiO_2-M systems [56] with the highest activity towards H_2 generation and acetic acid oxidation to CO_2 for samples containing anatase particles in the shell layer, pure ST01, and FP6 respectively. However, some differences were visible considering the exact value of the monitored process, with H_2 evolution being especially suppressed. On the other hand, the efficiency of acetic acid decomposition was promoted for Fe_3O4@SiO_2 surface coated with TiO_2 particles (Fig. 5b), which suggests that obtained magnetic nanocomposites are more suitable for oxidation processes rather than reduction due to the development of the specific surface area and formation of TiO_2-SiO_2 photocatalytic layer

for $Fe_3O_4@SiO_2/TiO_2$ nanocomposites in opposite to pure TiO_2 particles. For further confirmation of the presented thesis, additional measurements of photocatalytic activity in the reduction of 4-nitrophenol to 4-aminophenol as well as phenol oxidation reaction were performed. The described dependencies are shown in Figure 5 c,d. For phenol oxidation reaction, presented as constant rate k, the core-shell magnetic photocatalysts revealed significantly higher activity than pure TiO_2 matrices, while the opposite trend was observed for photoconversion of 4-nitrophenol to 4-aminophenol, with the highest efficiency for FP6 matrix.

Further differences were also observed for magnetic photocatalysts modified with Pt and Cu nanoparticles, as presented in Fig. 6 a,d.

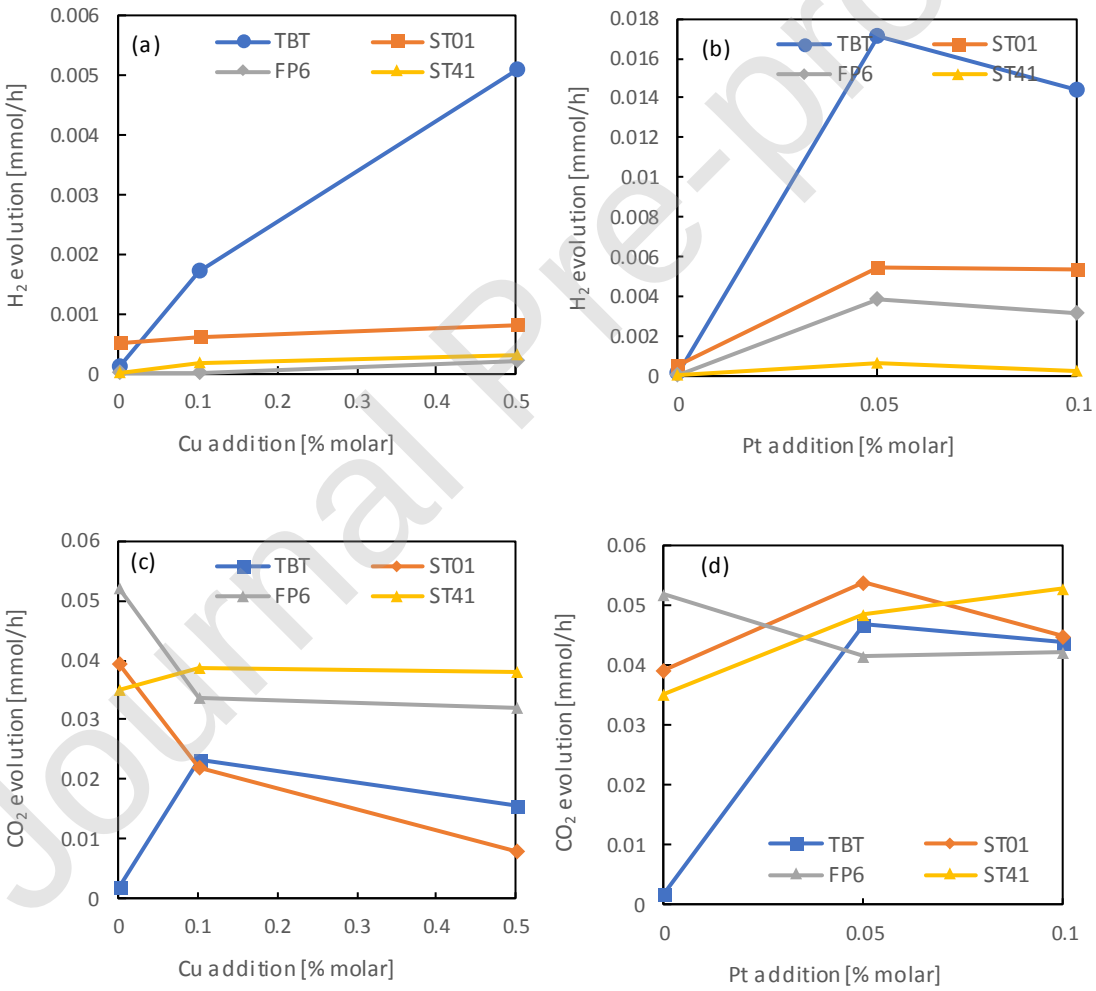

Fig. 6. The effect of metal loading on photocatalytic activity for: H_2 evolution (a-b), and acetic acid oxidation to CO_2 (CO_2 evolution) (c-d) for monometallic $Fe_3O_4@SiO_2/TiO_2$-M samples

Regarding H_2 evolution, a strong trend to promote the process in TBT-based systems was observed both for Cu and Pt modified samples; however, as presented in Fig. 6a-b, nearly ten times higher activity was observed for Pt-modified magnetic photocatalysts than for Cu-modified magnetic nanocomposites. Moreover, very little difference was observed between 0.05% and 0.1% platinum loading, which led to the observation that the metal presence, rather than its concentration, is the main factor affecting process efficiency in overall results. Regarding acetic acid degradation, the highest efficiency was observed for ST41 based samples, with no dependence on the character of the modification. In general, Cu presence decreased process efficiency in most cases, and pure FP6 matrices (a mixture of anatase and rutile) allowed to achieve a high degradation rate, while ST41 (anatase particles) synergizes with Pt nanoparticles. Moreover, TiO_2 particles obtained from TBT hydrolysis (fine anatase NPs), as well as, commercial TiO_2 ST01 consist also fine anatase particles modified with both Cu and Pt exhibited higher photoactivity than FP6 (mixture of anatase and rutile NPs) and ST41 (large anatase NPs), being weak or almost not affected by the presence of modifications. In the case of H_2 evolution, TiO_2 metal-modification allows to markedly improvement of process efficiency in Fe_3O_4@SiO_2/TBT core-shell systems since practically no activity was observed for samples without deposited metal nanoparticles (see in Figure 6). However, for acetic acid degradation, a strong matrix effect was observed, leading to the highest activity of ST41 and FP6 -based samples, despite them being less affected by both metals. Ultimately it can be stated that FP6 based composites, consists a mixture of anatase and rutile, possess the highest activity towards acetic acid degradation, while ST41 (large anatase NPs) achieved its maximum after modification with Pt nanoparticles only.Additional analyses were performed to evaluate the possible effect of combining Fe_3O_4@SiO_2 cores with TiO_2-M photocatalysts based on different TiO_2 matrices. It was found that both z2 (sample obtained by adding NH_4OH to TEOS), and z3 (sample obtained by addition of and TEOS/NH_4OH) are suitable for further modification, with

almost the same efficiency towards acetic acid degradation and some increase in H_2 generation in favor of z3 matrice, as shown in Fig. 7a-b.

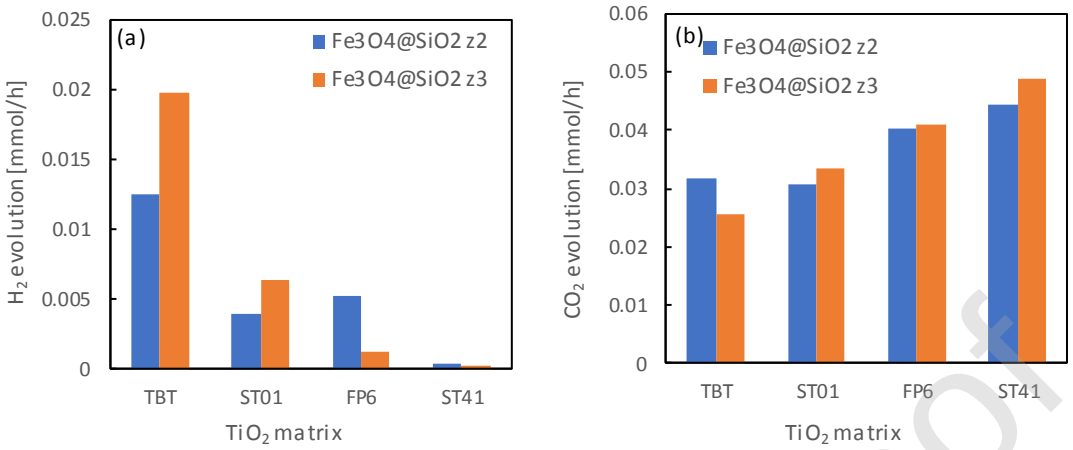

Fig. 7. H_2 (a) and acetic acid oxidation to CO_2 (b) for Fe_3O_4@SiO_2/TiO_2-M nanocomposites as a function of different Fe_3O_4@SiO_2 magnetic cores

Further analysis showed that the TBT-based photocatalyst layer in the structure of magnetic composite was especially active towards H_2 generation when combined with the z3 sample, while FP6 worked well with the z2 sample. Since, as presented in Data in Brief, TBT-based TiO_2-M photocatalysts were found to be favorable for H_2 production in general, this explains why in overall results, magnetic core material covered with TiO_2 anatase obtained from TBT (TBT shell samples) were more suitable and highly active in hydrogen evolution. On the other hand, no significant interactions between Fe_3O_4@SiO_2 magnetic samples and all TiO_2-M photocatalytic matrices were observed for acetic acid oxidation.

Finally, to confirm the observed dependencies, additional analyses of phenol oxidation were performed for mono- and bimetallic Fe_3O_4@SiO_2/TiO_2-M samples. Their overall results, presented as phenol degradation rate constant k and TOC removal, were compared with previously described acetic acid degradation efficiency. Obtained results, presented in Fig. 8 a-h, were in good agreement with the ones described for acetic acid, showing a high positive effect of Pt addition, together with its negative interactions with Cu and no impact of

Fe_3O_4@SiO_2 core selection. The selection of TiO_2 matrix also showed a similar impact to previously described. The highest activity was noticed for magnetic composites containing the photocatalyst layer of TiO_2 FP6 (a mixture of anatase and rutile) as well as TiO_2 ST41 (large anatase particles).

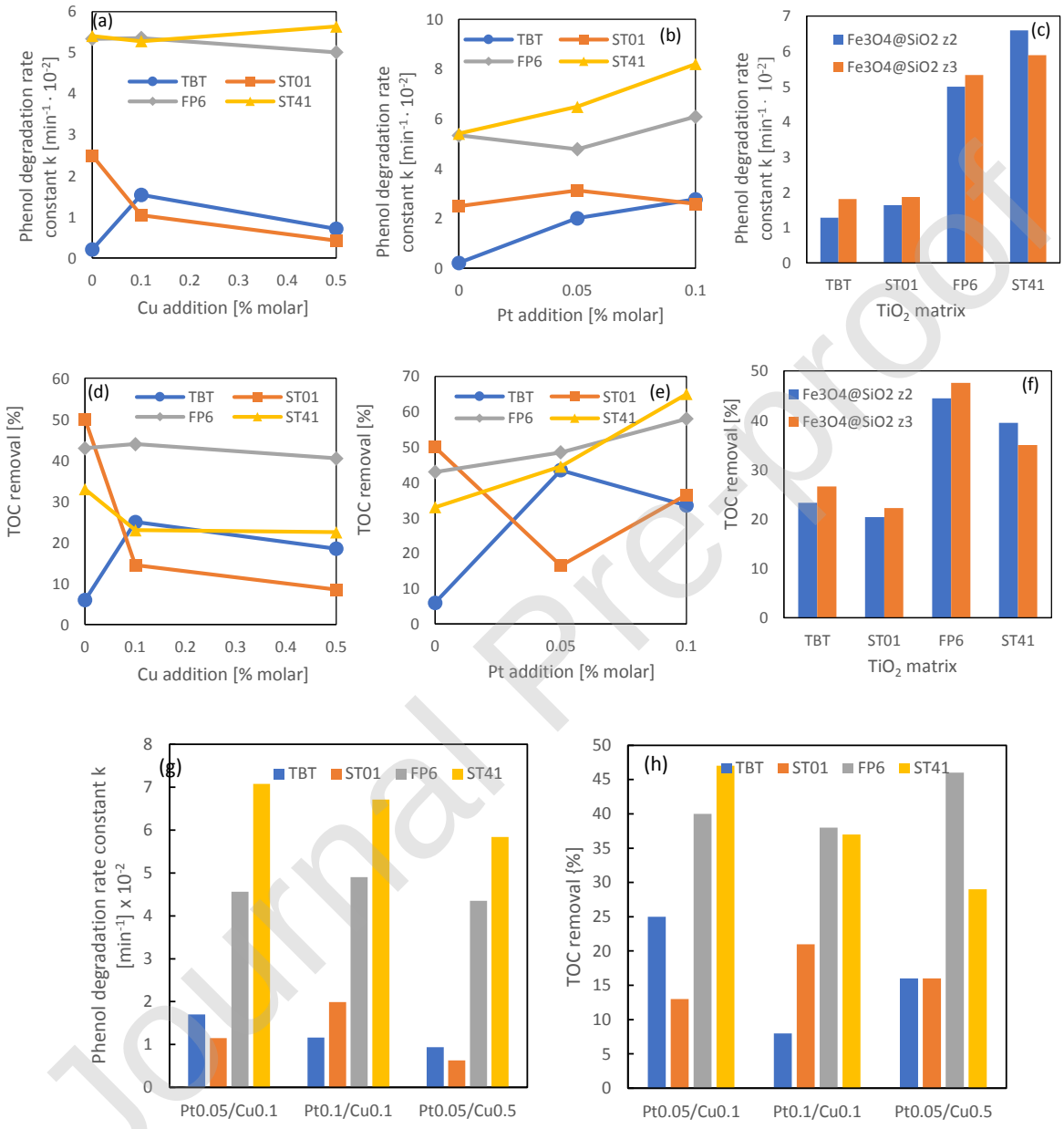

Fig. 8. Phenol degradation rate constant k and TOC removal for mono- (a-f) and bimetallic (g-h) nanocomposites. The effect of TiO_2 matrix, Fe_3O_4@SiO_2 matrices as well as Cu and Pt content.

Analyzed results are in good agreement with the study reported by Zielińska-Jurek et al. [68]. Large decahedral anatase particles (DAP) with crystalline size about 70 nm modified with 0.1 mol% of Pt nanoparticles exhibited the highest photocatalytic activity in phenol degradation reaction in UV-Vis irradiation range. It is also worth mentioning that Pt nanoparticles embedded on DAP surface were much bigger (17 nm) than nanoparticles on other TiO_2 matrices (ca. 5 nm). Similar high activity for ST41 TiO_2 was presented by Ohno et al. in the photocatalytic oxidation of adamantane [69]. Different situation was reported by Xie et al. [70] in their work regarding CO_2 reduction by various titania phases. Moreover, anatase/rutile and anatase/brookite mixed phases semiconductors could form a phase junction, where electrons could migrate from a higher conduction band (CB) to lower CB, promoting photogenerated charge carriers' separation [70–72]. Moreover, for methanol dehydrogenation the presence and properties of co-catalyst (noble metals) are the most crucial for being reaction centers [73].

3.3.Quantum efficiency analysis

The dependence of phenol degradation quantum efficiency on the irradiation wavelength (action spectrum) is presented in Fig. 9. Quantum efficiency was determined for mono- and bimetallic ST01-M and corresponding Fe_3O_4@SiO_2/ST01-M magnetic photocatalysts.

In the UV light range, the highest quantum yields were achieved by bimetallic photocatalysts, in which the ST01 surface was simultaneously modified with platinum and copper. For Fe_3O_4@SiO_2/ST01-M magnetic nanocomposites, bimetallic Fe_3O_4@SiO_2/ST01-Pt0.05/Cu0.1_z2 had almost twice as high performance as Fe_3O_4@SiO_2/ST01-Pt0.05_z2 (with only platinum in its structure). The ST01-Cu0.1 photocatalyst had the lowest quantum efficiency among the modified semiconductors. It is obvious that co-presence of platinum and copper results in a significant enhancement of Vis response. Although in the case of platinum, the mechanism is clear, i.e., platinum works as an electron sink (well-known since Bard studies [20]), the mechanism for copper-modified titania is not so obvious [74], including p-n junction,

Z-scheme electron transfer, Schottky barrier formation, and more complex charge carriers' transfer between various forms of copper (Cu_2O, CuO, Cu_xO, Cu) and titania. It has been proposed that Z-scheme electron transfer would be the most advisable (i.e., recombination of electrons from conduction band (CB) of titania with holes from valence band (VB) of copper oxides), resulting in highly reactive electrons in CB of copper oxides (more negative potential than that in titania) and holes in VB of titania (more positive potential than that in copper oxides) [18]. The present study suggests that in UV light range the co-presence of platinum might result in the formation of efficient Z-scheme photocatalyst., i.e., second-generation Z-scheme (all-solid-state (ASS) Z-scheme), in which platinum could work as an efficient conductor between copper oxide and titania [75].

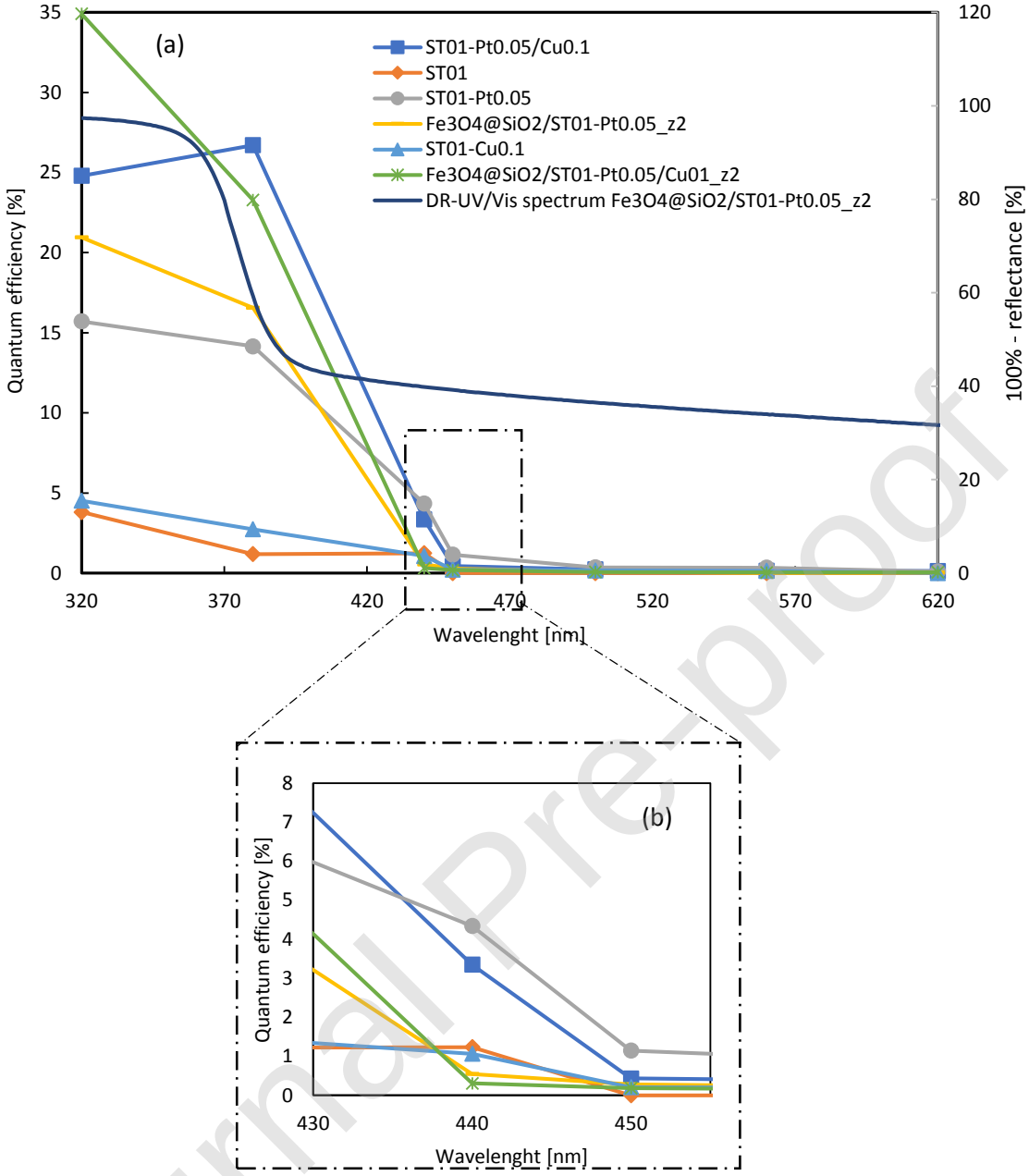

Fig. 9. Action spectra of phenol degradation for obtained nanocomposites: (a) at whole range of irradiation, and (b) at 430 - 455 nm field (magnification).

In the visible light range (> 420 nm), an apparent decrease in quantum efficiency was observed because of insufficient excitation of titania (absorption edge at ca. 400 nm). The slight activity even at 440 nm for bare titania could be explained by defects' presence, typical for almost all commercial titania samples ("self-doped" titania), which might result in slight Vis

response, i.e., excitation to/from defects (such defects have already been reported for ST01 at ca. 0-0.4 eV below CB bottom by reverse double-beam photoacoustic spectroscopy [76]). Platinum-modified samples showed the highest Vis activity confirming that plasmon resonance of platinum should activate titania [28]. Moreover, the Vis activity for magnetic composites was much lower comparing to TiO_2-M, which may result from competitive charge carriers' transfer between metal nanoparticles as well as titania. The previous study on hybrid photocatalysts (ruthenium complexes and plasmonic nanoparticles [77]) and some bimetallic photocatalysts (Au(core)/Ag(shell) [78]) indicated the enhanced charge carriers' recombination instead of their efficient separation in the case of photocatalysts modified by two modifiers. Based on our previous studies [28–30,68], the Pt particle size, which depends on (i) TiO_2 support type, (ii) reducing agent, (iii) annealing temperature, and (iv) metallic structure on TiO_2 support is crucial in Vis light activity. Therefore, the additional calcination of Fe_3O_4@SiO_2/TiO_2-M nanocomposites could have resulted in metal particles re-arrangement, their aggregation, and finally, in the observed lower photocatalytic activity compared to TiO_2-M photocatalysts.

3.4. Reusability of magnetic nanocomposites

The reusability of magnetic nanocomposites was studied in phenol degradation reaction in three subsequent cycles. Bimetallic Fe_3O_4@SiO_2/ST41-Pt0.05/Cu0.1_z2 was selected due to its excellent photocatalytic activity. After each 60 min cycle, nanocomposite was separated using a magnetic field and used in another run without any treatment. The obtained results are presented in Fig. 10. No loss in degradation was observed after three cycles of phenol degradation process. Thus, the magnetic nanocomposites revealed excellent stability and reusability.

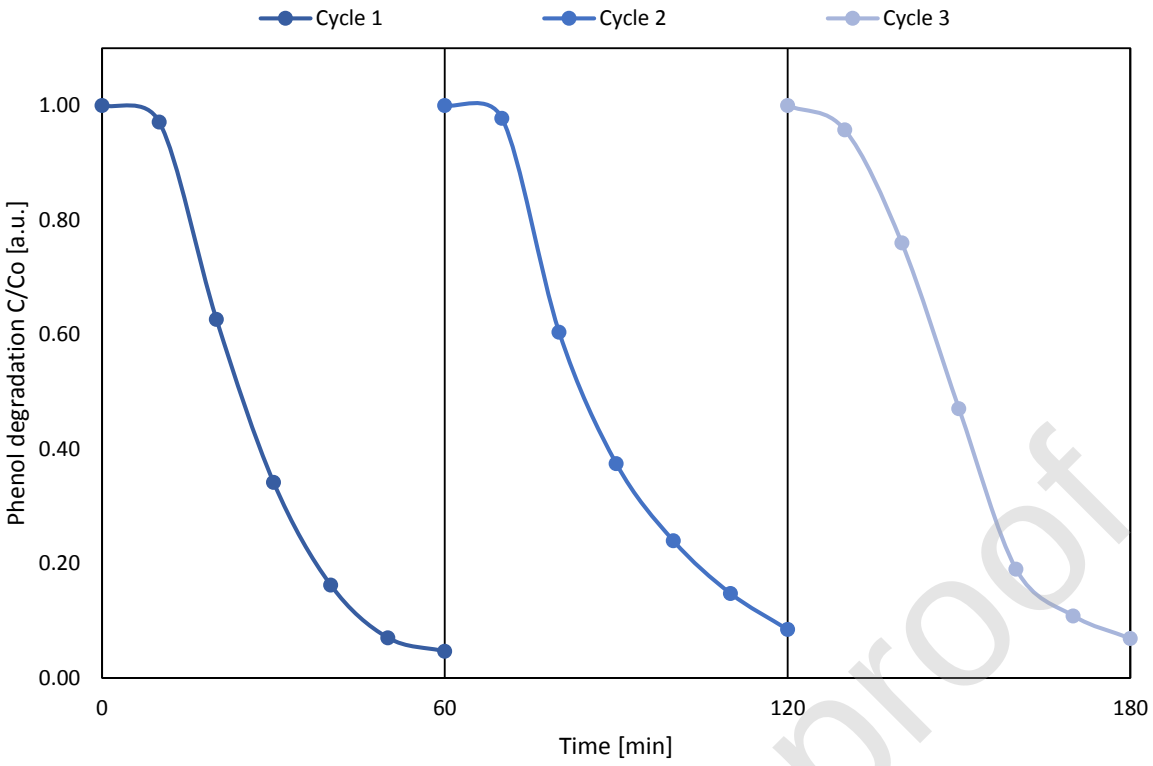

Fig. 10. Phenol degradation efficiency measured in three subsequent cycles in the presence of Fe_3O_4@SiO_2/ST41-Pt0.05/Cu0.1_z2

4. Conclusions

Mono- and bimetallic magnetic nanocomposites Fe_3O_4@SiO_2/TiO_2-M were successfully prepared using w/o microemulsion method. The core-interlayer-shell structure, where core was magnetic Fe_3O_4, inert interlayer was SiO_2, and a shell was composed of TiO_2 modified with Pt and Cu, allowed to increase both photocatalytic activity and separability. Action spectra for phenol decomposition correlated with corresponding absorption spectra for Pt-modified titania, and thus confirming that even its low content (0.05 mol%) could activate titania under Vis irradiation due to plasmon resonance of platinum. However, the co-existence of copper and platinum nanoparticles was beneficial only under UV light. In the Vis range decrease in activity was observed, suggesting that their co-deposition might work as charge carriers' recombination center. The most important finding was that introducing of magnetic nanoparticles as a core for

Fe_3O_4@SiO_2/TiO_2 and Fe_3O_4@SiO_2/TiO_2-M did not negatively influence the photocatalytic performance, as reported for immobilized photocatalysts. What is more, Fe_3O_4@SiO_2/TiO_2 revealed higher photocatalytic activity than pure TiO_2 in oxidation reactions (phenol and acetic acid decomposition). Moreover, along with excellent photocatalytic properties in the solar spectrum range, the outstanding stability, tested in three subsequent cycles of phenol decontamination, suggested the possibility of commercial application of magnetic nanocomposites for environmental purification.

CRediT author statement:

Zuzanna Bielan: Conceptualization, Visualization, Investigation, Writing-Original Draft

Ewa Kowalska: Supervision, Resources, Writing – Review and Editing

Szymon Dudziak: Formal analysis, Validation

Kunlei Wang: Investigation

Bunsho Ohtani: Supervision, Resources

Anna Zielińska-Jurek: Conceptualization, Supervision, Writing – Review and Editing

Declaration of interests

The authors declare that they have no known competing financial interests or personal relationships that could have appeared to influence the work reported in this paper.

Acknowledgements

This work was supported by the Polish National Science Centre (Grant No. NCN 2016/23/D/ST5/01021) and Gdansk University of Technology by InterPhD II (POWER) project (No. POWR.03.02.00-IP.08-00-DOK/16). Z.B. would like to highly acknowledge Dr. Maya Endo-Kimura from the Institute for Catalysis, Hokkaido University, Japan, for the inestimable help during conducting research.

References

[1] J.A. Fernandez, A. Suan, J.C. Ramirez, J. Robles, J.C. Salcedo, A.M. Pedroza, C.E. Daza, Treatment of real wastewater with TiO2-films sensitized by a natural-dye obtained from Picramnia sellowii, J. Environ. Chem. Eng. 4 (2016) 2848–2856. doi:10.1016/j.jece.2016.05.037.

[2] I. Wysocka, A. Markowska-Szczupak, P. Szweda, J. Ryl, M. Endo-Kimura, E. Kowlaska, G. Nowaczyk, A. Zielińska-Jurek, Gas- phase removal of indoor volatile organic compounds and airborne microorganisms over mono - and bimetal - modified (Pt , Cu , Ag) titanium(IV) oxide nanocomposites, Indoor Air. 00 (2019) 1–14. doi:10.1111/ina.12595.

[3] M. Matsuoka, M. Kitano, M. Takeuchi, K. Tsujimaru, M. Anpo, J.M. Thomas, Photocatalysis for new energy production. Recent advances in photocatalytic water splitting reactions for hydrogen production, Catal. Today. 122 (2007) 51–61. doi:10.1016/j.cattod.2007.01.042.

[4] A. Ofiarska, A. Pieczyńska, A. Fiszka Borzyszkowska, P. Stepnowski, E.M. Siedlecka, Pt-TiO2-assisted photocatalytic degradation of the cytostatic drugs ifosfamide and cyclophosphamide under artificial sunlight, Chem. Eng. J. 285 (2016) 417–427. doi:10.1016/j.cej.2015.09.109.

[5] A. Zielińska-Jurek, Z. Wei, I. Wysocka, P. Szweda, E. Kowalska, The effect of nanoparticles size on photocatalytic and antimicrobial properties of Ag-Pt/TiO<inf>2</inf> photocatalysts, Appl. Surf. Sci. 353 (2015) 317–325. doi:10.1016/j.apsusc.2015.06.065.

[6] M. Długokęcka, J. Łuczak, Ż. Polkowska, A. Zaleska-Medynska, The effect of microemulsion composition on the morphology of Pd nanoparticles deposited at the surface of TiO2 and photoactivity of Pd-TiO2, Appl. Surf. Sci. 405 (2017) 220–230. doi:10.1016/j.apsusc.2017.02.014.

[7] M. Klein, E. Grabowska, A. Zaleska, Noble metal modified TiO2 for photocatalytic air purification, Physicochem. Probl. Miner. Process. 51 (2015) 49–57.

[8] E. Grabowska, M. Marchelek, T. Klimczuk, G. Trykowski, A. Zaleska-Medynska, Noble metal modified TiO2 microspheres: surface properties and photocatalytic activity under UV–vis and visible light, J. Mol. Catal. A Chem. 423 (2016) 191–206. doi:10.1016/j.molcata.2016.06.021.

[9] E. Borowska, J.F. Gomes, R.C. Martins, R.M. Quinta-Ferreira, H. Horn, M. Gmurek, Solar Photocatalytic Degradation of Sulfamethoxazole by TiO2 Modified with Noble Metals, Catalysts. 9 (2019) 1–19.

[10] M. Endo, Z. Wei, K. Wang, B. Karabiyik, K. Yoshiiri, P. Rokicka, B. Ohtani, A. Markowska-Szczupak, E. Kowalska, Noble metal-modified titania with visible-light activity for the decomposition of microorganisms, Beilstein J. Nanotechnol. 9 (2018) 829–841. doi:10.3762/bjnano.9.77.

[11] H. Irie, Y. Watanabe, K. Hashimoto, Nitrogen-Concentration Dependence on Photocatalytic Activity of TiO2-xNx Powders, J. Phys. Chem. B. 107 (2003) 5483–5486.

[12] Y. Li, D. Hwang, H.N. Lee, S. Kim, Synthesis and characterization of carbon-doped titania as an artificial solar light sensitive photocatalyst, Chem. Phys. Lett. 404 (2005) 25–29. doi:10.1016/j.cplett.2005.01.062.

[13] L. Korosi, I. Dekany, Preparation and investigation of structural and photocatalytic properties of phosphate modified titanium dioxide, Colloids Surfaces A Physicochem. Eng. Asp. 280 (2006) 146–154. doi:10.1016/j.colsurfa.2006.01.052.

[14] S. Moon, H. Mametsuka, S. Tabata, E. Suzuki, Photocatalytic production of hydrogen from water using TiO2 and B/TiO2, Catal. Today. 58 (2000) 125–132.

[15] N. Rahimi, R.A. Pax, E.M.A. Gray, Review of functional titanium oxides. I: TiO2 and

its modifications, Prog. Solid State Chem. 44 (2016) 86–105. doi:10.1016/j.progsolidstchem.2016.07.002.

[16] J.C. Yu, J. Yu, W. Ho, Z. Jiang, L. Zhang, Effects of F-Doping on the Photocatalytic Activity and Microstructures of Nanocrystalline TiO2 Powders, Chem. Mater. 14 (2002) 3808–3816.

[17] M. Endo-Kimura, M. Janczarek, Z. Bielan, D. Zhang, K. Wang, A. Markowska-Szczupak, E. Kowalska, Photocatalytic and Antimicrobial Properties of Ag2O/TiO2 Heterojunction, ChemEngineering. 3 (2019) 1–18. doi:10.3390/chemengineering3010003.

[18] M. Janczarek, M. Endo, D. Zhang, K. Wang, E. Kowalska, Enhanced Photocatalytic and Antimicrobial Performance of Cuprous Oxide/Titania: The Effect of Titania Matrix, Materials (Basel). 11 (2018) 1–21. doi:10.3390/ma11112069.

[19] Z. Wang, X. Lang, Visible Light Photocatalysis of Dye-Sensitized TiO2: The Selective Aerobic Oxidation of Amines to Imines, Appl. Catal. B Environ. 224 (2018) 404–409. doi:10.1016/j.apcatb.2017.10.002.

[20] A.J. Bard, Photoelectrochemistry and heterogeneous photocatalysis at semiconductors, J. Photochem. 10 (1979) 59–75.

[21] E. Kowalska, R. Abe, B. Ohtani, Visible light-induced photocatalytic reaction of gold-modified titanium(IV) oxide particles: action spectrum analysis, Chem. Commun. 2 (2009) 241–243. doi:10.1039/b815679d.

[22] E. Kowalska, O.O. Prieto-Mahaney, R. Abe, B. Ohtani, Visible-light-induced photocatalysis through surface plasmon excitation of gold on titania surfaces, Phys. Chem. Chem. Phys. 12 (2010) 2344–2355. doi:10.1039/b917399d.

[23] X. Hou, J. Ma, A. Liu, D. Li, M. Huang, X. Deng, Visible light active TiO2 films prepared by electron beam deposition of noble metals, Nucl. Instrum. Methods Phys.

Res. B. 268 (2010) 550–554. doi:10.1016/j.nimb.2009.12.010.

[24] S. Sakthivel, M.V. Shankar, M. Palanichamy, B. Arabindoo, D.W. Bahnemann, V. Murugesan, Enhancement of photocatalytic activity by metal deposition: characterisation and photonic efficiency of Pt , Au and Pd deposited on TiO2 catalyst, Water Res. 38 (2004) 3001–3008. doi:10.1016/j.watres.2004.04.046.

[25] H. Fan, C. Lu, W.W. Lee, M. Chiou, C. Chen, Mechanistic pathways differences between P25-TiO2 and Pt-TiO2 mediated CV photodegradation, J. Hazard. Mater. 185 (2011) 227–235. doi:10.1016/j.jhazmat.2010.09.022.

[26] E. Kowalska, H. Remita, C. Colbeau-Justin, J. Hupka, J. Belloni, Modification of Titanium Dioxide with Platinum Ions and Clusters: Application in Photocatalysis, J. Phys. Chem. C. 112 (2008) 1124–1131.

[27] M. Ni, M.K.H. Leung, D.Y.C. Leung, K. Sumathy, A review and recent developments in photocatalytic water-splitting using TiO2 for hydrogen production, Renew. Sustain. Energy Rev. 11 (2007) 401–425. doi:10.1016/j.rser.2005.01.009.

[28] A. Zielińska-Jurek, A. Zaleska, Ag/Pt-modified TiO2 nanoparticles for toluene photooxidation in the gas phase, Catal. Today. 230 (2014) 104–111. doi:10.1016/j.cattod.2013.11.044.

[29] I. Wysocka, E. Kowalska, J. Ryl, G. Nowaczyk, A. Zielińska-Jurek, Morphology, Photocatalytic and Antimicrobial Properties of TiO2 Modified with Mono- and Bimetallic Copper , Platinum and Silver Nanoparticles, Nanomaterials. 9 (2019) 1–23.

[30] A. Zielińska-Jurek, Progress, Challenge, and Perspective of Bimetallic TiO2 -Based Photocatalysts, J. Nanomater. 2014 (2014) 1–17.

[31] Y. Shiraishi, H. Sakamoto, Y. Sugano, S. Ichikawa, T. Hirai, Pt-Cu Bimetallic Alloy Nanoparticles Supported on Anatase TiO2: Highly Active Catalysts for Aerobic Oxidation Driven by Visible Light, ACS Catal. 7 (2013) 9287–9297.

doi:10.1021/nn403954p.

[32] S. Shuang, R. Lv, Z. Xie, Z. Zhang, Surface Plasmon Enhanced Photocatalysis of Au/Pt-decorated TiO 2 Nanopillar Arrays, Sci. Rep. 6 (2016) 1–8. doi:10.1038/srep26670.

[33] C.F. Liriano-Jorge, U. Sohmen, A. Özkan, H. Gulyas, R. Otterpohl, TiO2 Photocatalyst Nanoparticle Separation: Flocculation in Different Matrices and Use of Powdered Activated Carbon as a Precoat in Low-Cost Fabric Filtration, Adv. Mater. Sci. Eng. 2014 (2014) 1–12.

[34] S.-A. Lee, K.-H. Choo, C.-H. Lee, H.-I. Lee, T. Hyeon, W. Choi, H.-H. Kwon, Use of Ultrafiltration Membranes for the Separation of TiO2 Photocatalysts in Drinking Water Treatment, Ind. Eng. Chem. Res. 40 (2001) 1712–1719.

[35] Q. Zhang, H. Wang, X. Fan, F. Lv, S. Chen, X. Quan, Fabrication of TiO2 nanofiber membranes by a simple dip-coating technique for water treatment, Surf. Coatings Technol. 298 (2016) 45–52. doi:10.1016/j.surfcoat.2016.04.054.

[36] A. Zielińska-Jurek, M. Klein, J. Hupka, Enhanced visible light photocatalytic activity of Pt/I-TiO2in a slurry system and supported on glass packing, Sep. Purif. Technol. 189 (2017) 246–252. doi:10.1016/j.seppur.2017.08.018.

[37] J.H. Wei, C.J. Leng, X.Z. Zhang, W.H. Li, Z.Y. Liu, J. Shi, Synthesis and magnetorheological effect of Fe3O4-TiO2 nanocomposite, J. Phys. Conf. Ser. 149 (2009) 25–29.

[38] X. Zhang, H. Wang, C. Yang, D. Du, Y. Lin, Preparation, characterization of Fe3O4 at TiO2 magnetic nanoparticles and their application for immunoassay of biomarker of exposure to organophosphorus pesticides, Biosens. Bioelectron. 41 (2013) 669–674. doi:10.1016/j.bios.2012.09.047.

[39] J. Wang, J. Yang, X. Li, D. Wang, B. Wei, H. Song, X. Li, S. Fu, Preparation and

photocatalytic properties of magnetically reusable Fe3O4@ZnO core/shell nanoparticles, Phys. E. 75 (2016) 66–71. doi:10.1016/j.physe.2015.08.040.

[40] T.A. Gad-Allah, S. Kato, S. Satokawa, T. Kojima, Treatment of synthetic dyes wastewater utilizing a magnetically separable photocatalyst (TiO2/SiO2/Fe3O4): Parametric and kinetic studies, Desalination. 244 (2009) 1–11. doi:10.1016/j.desal.2008.04.031.

[41] M.E. Hassan, Y. Chen, G. Liu, D. Zhu, J. Cai, Heterogeneous photo-Fenton degradation of methyl orange by Fe 2 O 3 / TiO 2 nanoparticles under visible light, J. Water Process Eng. 12 (2016) 52–57. doi:10.1016/j.jwpe.2016.05.014.

[42] R. Li, Y. Jia, N. Bu, J. Wu, Q. Zhen, Photocatalytic degradation of methyl blue using Fe2O3/TiO2 composite ceramics, J. Alloys Compd. 643 (2015) 88–93. doi:10.1016/j.jallcom.2015.03.266.

[43] W. Fu, H. Yang, M. Li, L. Chang, Q. Yu, J. Xu, G. Zou, Preparation and photocatalytic characteristics of core-shell structure TiO2/BaFe12O19 nanoparticles, Mater. Lett. 60 (2006) 2723–2727. doi:10.1016/j.matlet.2006.01.078.

[44] F. Bavarsiha, M. Rajabi, M. Montazeri-Pour, Synthesis of SrFe12O19/SiO2/TiO2 composites with core/shell/shell nano-structure and evaluation of their photo-catalytic efficiency for degradation of methylene blue, J. Mater. Sci. Mater. Electron. 29 (2018) 1877–1887. doi:10.1007/s10854-017-8098-5.

[45] S.W. Lee, J. Drwiega, C.Y. Wu, D. Mazyck, W.M. Sigmund, Anatase TiO2 Nanoparticle Coating on Barium Ferrite Using Titanium Bis-Ammonium Lactato Dihydroxide and Its Use as a Magnetic Photocatalyst, Chem. Mater. 16 (2004) 1160–1164. doi:10.1021/cm0351902.

[46] X. Li, D. Liu, S. Song, H. Zhang, Fe3O4@SiO2@TiO2@Pt Hierarchical Core−Shell Microspheres: Controlled Synthesis, Enhanced Degradation System, and Rapid

Magnetic Separation to Recycle, Cryst. Growth Des. 14 (2014) 5506–5511. doi:10.1021/cg501164c.

[47] J. Zhan, H. Zhang, G. Zhu, Magnetic photocatalysts of cenospheres coated with Fe3O 4/TiO2 core/shell nanoparticles decorated with Ag nanopartilces, Ceram. Int. 40 (2014) 8547–8559. doi:10.1016/j.ceramint.2014.01.069.

[48] L. Zhang, Z. Wu, L. Chen, L. Zhang, X. Li, H. Xu, H. Wang, G. Zhu, Preparation of magnetic Fe3O4/TiO2/Ag composite microspheres with enhanced photocatalytic activity, Solid State Sci. 52 (2016) 42–48. doi:10.1016/j.solidstatesciences.2015.12.006.

[49] G. Liu, F. He, J. Zhang, L. Li, F. Li, L. Chen, Y. Huang, Yolk-shell structured Fe3O4CF-TiO2 microspheres with surface fluorinated as recyclable visible-light driven photocatalysts, Appl. Catal. B Environ. 150–151 (2014) 515–522. doi:10.1016/j.apcatb.2013.12.050.

[50] F. Shi, Y. Li, Q. Zhang, H. Wang, Synthesis of Fe3O4/C/TiO2 magnetic photocatalyst via vapor phase hydrolysis, Int. J. Photoenergy. 2012 (2012). doi:10.1155/2012/365401.

[51] T.A. Gad-Allah, S. Kato, S. Satokawa, T. Kojima, Role of core diameter and silica content in photocatalytic activity of TiO2/SiO2/Fe3O4 composite, Solid State Sci. 9 (2007) 737–743. doi:10.1016/j.solidstatesciences.2007.05.012.

[52] J. Cui, T. He, X. Zhang, Synthesis of Fe3O4@SiO2@Ption–TiO2 hybrid composites with high efficient UV–visible light photoactivity, Catal. Commun. 40 (2013) 66–70. doi:10.1016/j.catcom.2013.06.009.

[53] H. Liu, Z. Jia, S. Ji, Y. Zheng, M. Li, H. Yang, Synthesis of TiO2/SiO2@Fe3O4 magnetic microspheres and their properties of photocatalytic degradation dyestuff, Catal. Today. 175 (2011) 293–298. doi:10.1016/j.cattod.2011.04.042.

[54] X. Yan, T. Ohno, K. Nishijima, R. Abe, B. Ohtani, Is methylene blue an appropriate substrate for a photocatalytic activity test? A study with visible-light responsive titania, Chem. Phys. Lett. 429 (2006) 606–610. doi:10.1016/j.cplett.2006.08.081.

[55] N. Barbero, D. Vione, Why Dyes Should Not Be Used to Test the Photocatalytic Activity of Semiconductor Oxides, Environ. Sci. Technol. 50 (2016) 2130–2131. doi:10.1021/acs.est.6b00213.

[56] Z. Bielan, E. Kowalska, S. Dudziak, K. Wang, B. Ohtani, A. Zielinska-Jurek, Mono- and bimetallic (Pt/Cu) titanium(IV) oxide photocatalysts. Physicochemical and photocatalytic data for magnetic nanocomposites' shell, Data Br. (n.d.).

[57] A. Zielińska-Jurek, Z. Bielan, S. Dudziak, I. Wolak, Z. Sobczak, T. Klimczuk, G. Nowaczyk, J. Hupka, Design and Application of Magnetic Photocatalysts for Water Treatment. The Effect of Particle Charge on Surface Functionality, Catalysts. 7 (2017) 1–18. doi:10.3390/catal7120360.

[58] I. Wysocka, E. Kowalska, K. Trzciński, M. Łapiński, G. Nowaczyk, A. Zielińska-Jurek, UV-Vis-Induced Degradation of Phenol over Magnetic Photocatalysts Modified with Pt , Pd , Cu and Au Nanoparticles, Nanomaterials. 8 (2018) 1–20. doi:10.3390/nano8010028.

[59] K. Imamura, T. Yoshikawa, K. Hashimoto, H. Kominami, Environmental Stoichiometric production of aminobenzenes and ketones by photocatalytic reduction of nitrobenzenes in secondary alcoholic suspension of titanium(IV) oxide under metal-free conditions, Appl. Catal. B Environ. 134–135 (2013) 193–197. doi:10.1016/j.apcatb.2013.01.015.

[60] V. Brezova, A. Blazkova, I. Surina, B. Havlinova, Solvent effect on the photocatalytic reduction of 4-nitrophenol in titanium dioxide suspensions, J. Photochem. Photobiol. A Chem. 107 (1997) 233–237.

[61] A. Di Paola, M. Bellardita, L. Palmisano, Brookite, the Least Known TiO2 Photocatalyst, Catalysts. 3 (2013) 36–73. doi:10.3390/catal3010036.

[62] Y. Chi, Q. Yuan, Y. Li, L. Zhao, N. Li, X. Li, W. Yan, Magnetically separable Fe3O4@SiO2@TiO2-Ag microspheres with well-designed nanostructure and enhanced photocatalytic activity, J. Hazard. Mater. 262 (2013) 404–411. doi:10.1016/j.jhazmat.2013.08.077.

[63] E. Mrotek, S. Dudziak, I. Malinowska, D. Pelczarski, Z. Ryżyńska, A. Zielińska-Jurek, Improved degradation of etodolac in the presence of core-shell ZnFe2O4/SiO2/TiO2 magnetic photocatalyst, Sci. Total Environ. 724 (2020) 1–12. doi:10.1016/j.scitotenv.2020.138167.

[64] Y. Shiraishi, D. Tsukamoto, Y. Sugano, A. Shiro, S. Ichikawa, S. Tanaka, T. Hirai, Platinum Nanoparticles Supported on Anatase Titanium Dioxide as Highly Active Catalysts for Aerobic Oxidation under Visible Light Irradiation, ACS Catal. 2 (2012) 1984–1992. doi:10.1021/cs300407e.

[65] Z. Wei, M. Endo, K. Wang, E. Charbit, A. Markowska-szczupak, B. Ohtani, E. Kowalska, Noble metal-modified octahedral anatase titania particles with enhanced activity for decomposition of chemical and microbiological pollutants, Chem. Eng. J. 318 (2017) 121–134. doi:10.1016/j.cej.2016.05.138.

[66] M. Janczarek, Z. Wei, M. Endo, B. Ohtani, E. Kowalska, Silver- and copper-modified decahedral anatase titania particles as visible light-responsive plasmonic photocatalyst, J. Photonics Energy. 7 (2016) 1–16. doi:10.1117/1.JPE.7.012008.

[67] I. Krivtsov, M. Ilkaeva, E. Salas-Colera, Z. Amghouz, J.R. Garc, E. Diaz, S. Ordonez, S. Villar-Rodil, Consequences of Nitrogen Doping and Oxygen Enrichment on Titanium Local Order and Photocatalytic Performance of TiO2 Anatase, J. Phys. Chem. C. 121 (2017) 6770–6780. doi:10.1021/acs.jpcc.7b00354.

[68] A. Zielińska-Jurek, Z. Wei, M. Janczarek, I. Wysocka, E. Kowalska, Size- Controlled Synthesis of Pt Particles on TiO2 Surface: Physicochemical Characteristic and Photocatalytic Activity, Catalysts. 9 (2019) 1–18. doi:10.3390/catal9110940.

[69] T. Ohno, M. Akiyoshi, T. Umebayashi, K. Asai, T. Mitsui, M. Matsumura, Preparation of S-doped TiO2 photocatalysts and their photocatalytic activities under visible light, Appl. Catal. A Gen. 265 (2004) 115–121. doi:10.1246/cl.2003.364.

[70] S. Xie, Q. Zhang, G. Liu, Y. Wang, Photocatalytic and photoelectrocatalytic reduction of CO2 using heterogeneous catalysts with controlled nanostructures, Chem. Commun. 52 (2016) 35–59. doi:10.1039/C5CC07613G.

[71] J. Zhang, Q. Xu, Z. Feng, M. Li, C. Li, Importance of the Relationship between Surface Phases and Photocatalytic Activity of TiO2, Angew. Chemie. 47 (2008) 2006–2009. doi:10.1002/anie.200704788.

[72] G. Li, S. Ciston, Z. V. Saponjic, L. Chen, N.M. Dimitrijevic, T. Rajh, K.A. Gray, Synthesizing mixed-phase TiO2 nanocomposites using a hydrothermal method for photo-oxidation and photoreduction applications, J. Catal. 253 (2008) 105–110. doi:10.1016/j.jcat.2007.10.014.

[73] K. Wang, Z. Wei, B. Ohtani, E. Kowalska, Interparticle electron transfer in methanol dehydrogenation on platinum- loaded titania particles prepared from P25, Catal. Today. 303 (2018) 327–333. doi:10.1016/j.cattod.2017.08.046.

[74] M. Janczarek, E. Kowalska, On the Origin of Enhanced Photocatalytic Activity of Copper- Modified Titania in the Oxidative Reaction Systems, Catalysts. 7 (2017) 1–26. doi:10.3390/catal7110317.

[75] J. Low, C. Jiang, B. Cheng, S. Wageh, A.A. Al-ghamdi, J. Yu, A Review of Direct Z-Scheme Photocatalysts, Small Methods. 1 (2017) 1700080–1700101. doi:10.1002/smtd.201700080.

[76] K. Wang, M. Endo-Kimura, R. Belchi, D. Zhang, A. Habert, J. Boucle, B. Ohtani, E. Kowalska, N. Herlin-Boime, Carbon/Graphene-Modified Titania with Enhanced Photocatalytic Activity under UV and Vis Irradiation, Materials (Basel). 12 (2019) 1–19.

[77] E. Kowalska, K. Yoshiiri, Z. Wei, S. Zheng, E. Kastl, H. Remita, B. Ohtani, S. Rau, Hybrid photocatalysts composed of titania modified with plasmonic nanoparticles and ruthenium complexes for decomposition of organic compounds, App. Catal. B Environ. 178 (2015) 133–143.

[78] E. Kowalska, Z. Wei, B. Karabiyik, A. Herissan, M. Janczarek, M. Endo, H. Remita, B. Ohtani, Silver-modified titania with enhanced photocatalytic and antimicrobial properties under UV and visible light irradiation, Catal. Today. 252 (2015) 136–142. doi:10.1016/j.cattod.2014.10.038.